


 Cite this: *New J. Chem.*, 2023, **47**, 4510

Assessing the role of substituents in ferrocene acylphosphines and their impact on gold-catalysed reactions†

 Petr Vosáhl^o  and Petr Štěpnička *

Substituents can be used to efficiently modify the coordination and catalytic behaviour of phosphine ligands. In this article, we analyse how substituents affect the properties of ferrocene acylphosphines FcC(O)PR_2 (**1a–d**), where PR_2 is PPh_2 (**1a**), PCy_2 (**1b**), PAD_2 (**1c**) and PCg (**1d**; Fc = ferrocenyl, Cy = cyclohexyl, Ad = 1-adamantyl, and PCg = 1,3,5,7-tetramethyl-2,4,6-trioxa-8-phosphaadamantane-8-yl). The ^{31}P – ^{77}Se scalar coupling constants ($^1J_{\text{PSe}}$), determined for the corresponding phosphine selenides FcC(O)P(Se)R_2 (**2a–d**), suggest that the basicity of the phosphine groups increases with the donor ability of the substituents R, as expected. Au(I) complexes $[\text{AuCl}(\text{1-}\kappa\text{P})]$ (**3a–d**), obtained by replacing the dimethylsulfide ligand in $[\text{AuCl}(\text{SMe}_2)]$ with acylphosphines **1a–d**, were tested in Au-catalysed alkyne hydration and intramolecular cyclisation of *N*-propargyl benzamide to yield 5-methylene-2-phenyl-4,5-dihydrooxazole. The collected results indicate that the highest reaction yields were generally obtained using catalysts derived from acylphosphines bearing the electron-donating aliphatic substituents **1b** and **1c**. From a wider perspective, the carbonyl moiety in the acylphosphines FcC(O)PR_2 appears to lower steric crowding around the phosphorus atom (especially for compounds with bulky R substituents) and counterbalances the electron-donating effect of the ferrocenyl moiety.

 Received 13th January 2023,
 Accepted 3rd February 2023

DOI: 10.1039/d3nj00201b

rsc.li/njc

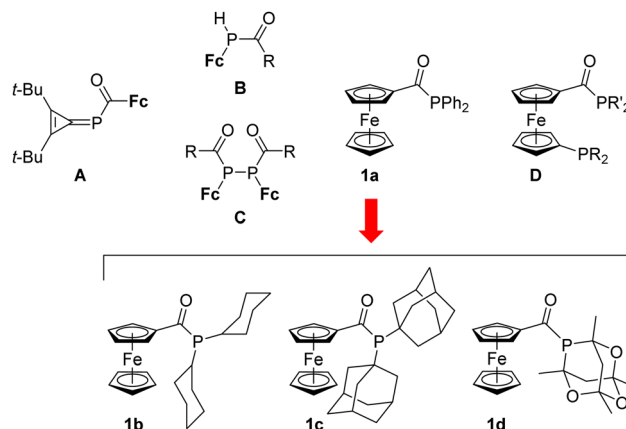
Introduction

Tertiary acylphosphines, $\text{RC(O)PR}'_2$, have emerged as alternatives to conventional triorganophosphine ligands.^{1,2} However, such compounds remain rare among the widely studied ferrocene phosphines.³ Thus, the triafulvene derivative **A** (Scheme 1), a rather obscure ferrocene acylphosphine, was reported in 1991.⁴ The more conventional compounds, **B** and **C**, accessible from alkylidene phosphines $\text{FcP}=\text{CR}(\text{OSiMe}_3)$, followed in 1997.⁵ More recently,⁶ we reported the synthesis of ferrocene acylphosphine FcC(O)PPh_2 (**1a**; Scheme 1) and its facile orthopalladation, which differentiates this compound from its conventional counterpart, (diphenylphosphino)ferrocene (FcPPh_2). Subsequently, we also prepared a series of monoacyl diphosphines, $\text{R}_2\text{PfcC(O)PR}'_2$ (**A**; R/R' = Ph and cyclohexyl (Cy); all possible combinations),⁷ which are analogues of the widely studied 1,1'-(diphenylphosphino)ferrocene (dppf),⁸ and compared the coordination and catalytic properties of these compounds.

Department of Inorganic Chemistry, Faculty of Science, Charles University, Hlavova, 2030, 128 40 Prague, Czech Republic. E-mail: petr.stepnicka@natur.cuni.cz

† Electronic supplementary information (ESI) available: Additional structural diagrams, summary of the crystallographic parameters and copies of the NMR spectra. CCDC 2235366–2235370. For ESI and crystallographic data in CIF or other electronic format see DOI: <https://doi.org/10.1039/d3nj00201b>

In continuation of these studies, we are currently investigating the properties and catalytic behaviour of ligands related to compound **1a**. In particular, we report the syntheses of three additional compounds of this type bearing different substituents at the phosphorus atom, *viz.* FcC(O)PCy_2 (**1b**; Cy = cyclohexyl), FcC(O)PAD_2 (**1c**, Ad = 1-adamantyl) and the “cage” phosphine,^{9,10} FcC(O)PCg (**1c**, PCg = 1,3,5,7-tetramethyl-2,4,6-trioxa-8-phosphaadamantane-8-yl).



Scheme 1 Ferrocene acylphosphines **1a**, **A–D** (in **B** and **C**: R = Fc, Ph, and *t*-Bu; Fc = ferrocenyl) and newly prepared compounds **1b–d**.



These compounds were used to prepare corresponding phosphine selenides and Au(I) complexes [AuCl(L-κP)] (L = **1a–d**). The gold complexes were further studied as defined precatalysts in two model gold-catalysed reactions, namely, the hydration of terminal alkynes and cyclisation of *N*-propargylbenzamide to 2-phenyl-5-methyleneoxazoline, and the catalytic results were analysed in terms of the ligand properties.

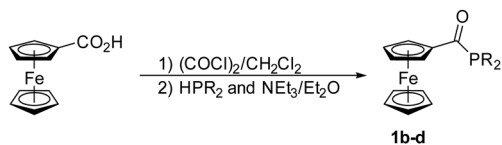
Results and discussion

Syntheses and characterisation

The acylphosphines **1b–d** (Scheme 2) were obtained similarly to **1a**⁶ using the following one-pot procedure: ferrocenecarboxylic acid was initially reacted with oxalyl chloride to provide ferrocenecarbonyl chloride, and the formed acyl chloride was directly reacted with the respective secondary phosphine in the presence of triethylamine as an HCl scavenger. The reaction with dicyclohexylphosphine was clean and rapid and afforded **1b** in a 93% yield after simple chromatographic purification. An analogous reaction employing di(1-adamantyl)phosphine required a longer reaction time and a modified workup procedure because both the secondary phosphine and **1c** were only sparingly soluble in diethyl ether used as a solvent during the second reaction step, and the product separated out of the reaction mixture along with (Et₃NH)Cl. Therefore, the reaction mixture was evaporated, and the residue was partitioned between dichloromethane and water. Subsequent chromatography afforded pure **1c** in an average 54% yield. Longer reaction times were also required to prepare compound **1d** bearing 1,3,5,7-tetramethyl-2,4,6-trioxa-8-phosphaadamantane-8-yl group. Purification by chromatography and crystallisation from pentane afforded **1d** in a 17% yield. Such a low isolated yield reflects low solubility and reactivity of the electron-poor phosphine HPCg and high solubility of the acylphosphine.

Compounds **1b–d** were obtained as burgundy red solids, which could be stored in air for months without any observable decomposition and were characterised by NMR and IR spectroscopy, ESI MS and elemental analysis. In addition, the structure of **1c** was determined by single-crystal X-ray diffraction analysis.

The ³¹P chemical shifts of the acylphosphines are given in Table 1. The ¹H and ¹³C NMR spectra of the compounds exhibited the characteristic signals of phosphine substituents and the ferrocene unit, namely a C₅H₅ singlet and two multiplets due to C₅H₄ in the ¹H NMR spectra and resonances from three CHs and one C^{ipso} in the ¹³C NMR spectra. The signals of the carbonyl group were observed as phosphorus-coupled doublets at δ_C 210–220. A downfield shift of the C=O resonances with



Scheme 2 Preparation of **1b–d** (**b**: PR₂ = PCy₂, **c**: PR₂ = PAD₂, **d**: PR₂ = PCg; Cy = cyclohexyl, Ad = 1-adamantyl, and PCg = 1,3,5,7-tetramethyl-2,4,6-trioxa-8-phosphaadamantane-8-yl; see Scheme 1).

Table 1 Summary of the ³¹P NMR parameters for **1–3**^a

Compound	δ _P [¹ J _{PSe}]		
	L (1a–d)	L=Se (2a–d)	[AuCl(L-κP)] (3a–d)
FcC(O)PPh ₂ (a)	11.0 ^b	28.2 [749] ^b	29.3
FcC(O)PCy ₂ (b)	17.8	52.3 [718]	45.0
FcC(O)PAD ₂ (c)	45.3	68.2 [709]	64.1
FcC(O)PCg (d)	−14.5	24.2 [761]	16.0

^a The spectra were recorded in CDCl₃ at 25 °C. The chemical shifts are reported in ppm with respect to 85% H₃PO₄, and the coupling constants are given in Hz. ^b Data from ref. 6.

respect to ferrocenecarboxylic acid (δ_C 177.6)¹¹ and analogous amides (*cf.* δ_C 160.5 for FcC(O)NCy₂ and 171.2 for FcC(O)NPh₂)¹² suggests a lower carbonyl-heteroatom conjugation in **1b–d**. Carbonyl stretching bands in the IR spectra of **1b–d** appeared in the 1606–1616 cm^{−1} range (*cf.* ν_{C=O} 1609 cm^{−1} for **1a**). These values are difficult to compare with the data for the corresponding amides because IR spectra may change with the condensation state and experimental setup (neat or dispersed samples).

The molecular structure of **1c** and selected geometric data are presented in Fig. 1. The structure comprises unperturbed ferrocene unit. The C=O bond is twisted by 9.5(5)° from the plane of its parent cyclopentadienyl ring C(1–5), which is further manifested by the torsion angles C2–C1–C11–O and C5–C1–C11–O of −168.3(5) and 6.0(8)°, respectively. The C=O bond length in **1c** (1.228(7) Å) is practically identical to that in **1a** (1.225(2) Å).⁶ However, **1c** has longer P–C(Ad) bonds than the mentioned reference compound, which is in line with the lack of conjugation and higher steric demands of the adamantyl substituents. Correspondingly, the C12–P–C22 angle is the largest of the C–P–C angles.

To compare the “electronic” properties (basicity) of the prepared ligands,¹³ the acylphosphines **1b–d** were treated with

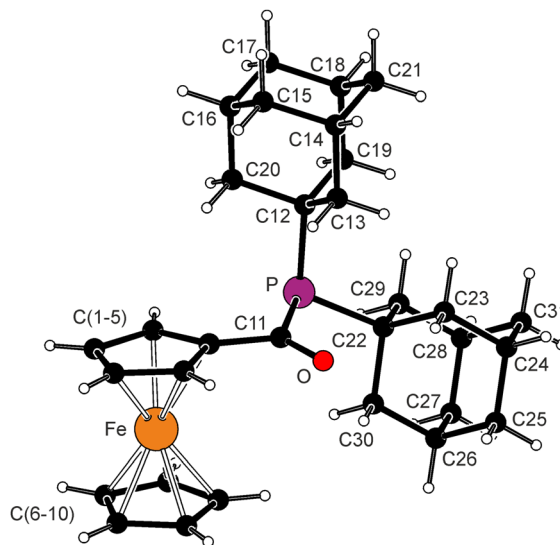
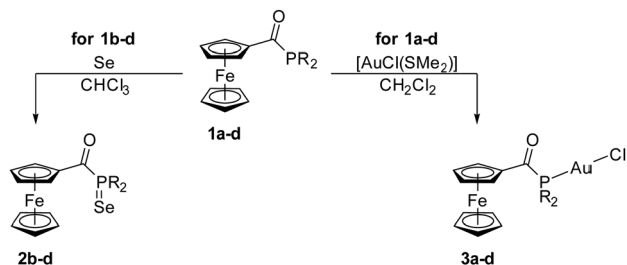


Fig. 1 Structure diagram for **1c**. Selected distances and angles (in Å and deg): Fe–C(1–10) 2.029(7)–2.053(5), dihedral angle of the cyclopentadienyl planes 2.5(3), C11=O 1.228(7), P–C11 1.882(6), P–C12 1.895(5), P–C22 1.884(6), C1–C11–P 115.3(4), C11–P–C12 97.4(2), C11–P–C22 102.3(2), and C12–P–C22 112.4(2).





Scheme 3 Synthesis of the phosphine selenides **2** and Au(I) complexes **3**.

grey selenium in refluxing chloroform to give the respective phosphine selenides **2b–d** (Scheme 3). The selenation reactions proceed cleanly and with full conversions. Thus, the isolated yields mainly reflected the efficacy of the crystallisation procedure used to isolate the compounds (yields: 66% for **2b**, 85% for **2c**, and 53% for **2d**).

The selenylation of the phosphines resulted in a low-field shift of the ^{31}P NMR signals and the appearance of characteristic ^{77}Se satellites ($I = 1/2$, natural abundance: 7.6%). The ^{13}C NMR resonances due to the carbonyl groups were also downfield-shifted ($\Delta\delta_{\text{C}} \approx 12$ ppm), reflecting the high electron-withdrawing abilities of the $\text{P}(\text{Se})\text{R}_2$ substituents.

The $^1J_{\text{PSe}}$ scalar coupling constants of phosphine selenides are directly proportional to the pK_{B} of the parent phosphines, 14 such that larger $^1J_{\text{PSe}}$ values indicate a lower Brønsted basicity. However, steric factors must also be considered, 14,15 especially for bulky phosphines, because the s -character of the P–Se bond that determines the $^1J_{\text{PSe}}$ coupling constant changes with the C–P–C angles. In the present case, however, steric factors appear to play a minor role due to the presence of the C=O linker.

The $^1J_{\text{PSe}}$ values of **2a–d**, which are compiled in Table 1 and compared in Fig. 2, suggest that compounds **1a–d** cover a wide basicity range, whereas the trend in the $^1J_{\text{PSe}}$ values of $\mathbf{2c} < \mathbf{2b} < \mathbf{2a} < \mathbf{2d}$ reflects the electron-donating ability of the phosphine substituents. 16 Furthermore, the increase in $^1J_{\text{PSe}}$ from the “simple” phosphine FcPR_2 ($\text{R} = \text{Ph}$, $^1J_{\text{PSe}} = 735$ Hz; $\text{R} = \text{Cy}$, $^1J_{\text{PSe}} = 700$ Hz) 17 to the corresponding acylphosphine $\text{FcC}(\text{O})\text{PR}_2$ ($\Delta^1J_{\text{PSe}} \approx 17$ Hz) indicates that the carbonyl group inserted between the phosphine moiety and the electron-donating ferrocenyl substituent significantly lowers the basicity (σ -donor ability) of the phosphorus atom.

Fig. 2 presents a wider comparison, showing that the introduced carbonyl moiety neutralises (at least partially) the electron-donating effect of the ferrocenyl group (*cf.* the $^1J_{\text{PSe}}$ values for FcPPh_2 and FcPCy_2). As such, $\text{FcC}(\text{O})$ and additional substituents allow modification of the ligand basicity in both directions from that of the archetypal phosphine PPh_3 .

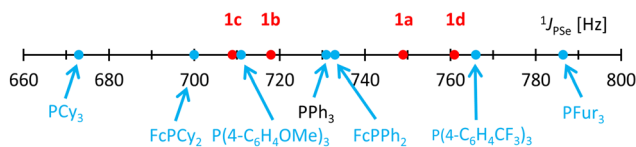


Fig. 2 Graphical comparison of the $^1J_{\text{PSe}}$ values for phosphine selenides **1c–d** and related compounds. 18

The solid-state structures of the selenides **2b–d** are shown in Fig. 3, and selected geometric data are presented in Table 2. All structures contain regular ferrocene units with negligibly tilted cyclopentadienyl rings ($\leq 2^\circ$). The C1–C11–P angles are close to 120° , as expected for an sp^2 carbon ($120\text{--}123^\circ$ in the series), and the acylphosphine fragment $\{\text{C11}, \text{P}, \text{O1}\}$ is tilted with respect to the bonding cyclopentadienyl ring $\text{C}(1\text{--}5)$ by $3.5(1)^\circ$ in **2b**, $1.4(2)^\circ$ in **2c**, and $9.3(1)^\circ$ in **2d**. The P=Se distances in **2b–d** are mutually similar and compare well with the value for **2a** ($2.1035(7)$ Å). 6 Finally, a comparison of the parameters determined for the pairs **1a–2a** and **1c–2c** reveals a slight opening of the C–P–C angles upon selenylation.

Compounds **1a–d** were treated with stoichiometric quantities of $[\text{AuCl}(\text{SMe}_2)]$ to produce the corresponding gold(I)–phosphine complexes $[\text{AuCl}(\text{1-}\kappa\text{P})]$ (**3a–d**) (Scheme 3), which were isolated as deep burgundy red solids in good yields (74–85%) after crystallisation or flash chromatography. While stable as solids, the compounds slowly decomposed in solution upon exposure to daylight, depositing a violet precipitate and gold mirror. Coordination to the AuCl fragment resulted in a downfield shift of the ^{31}P NMR signals (by 18–30 ppm in the series) and the

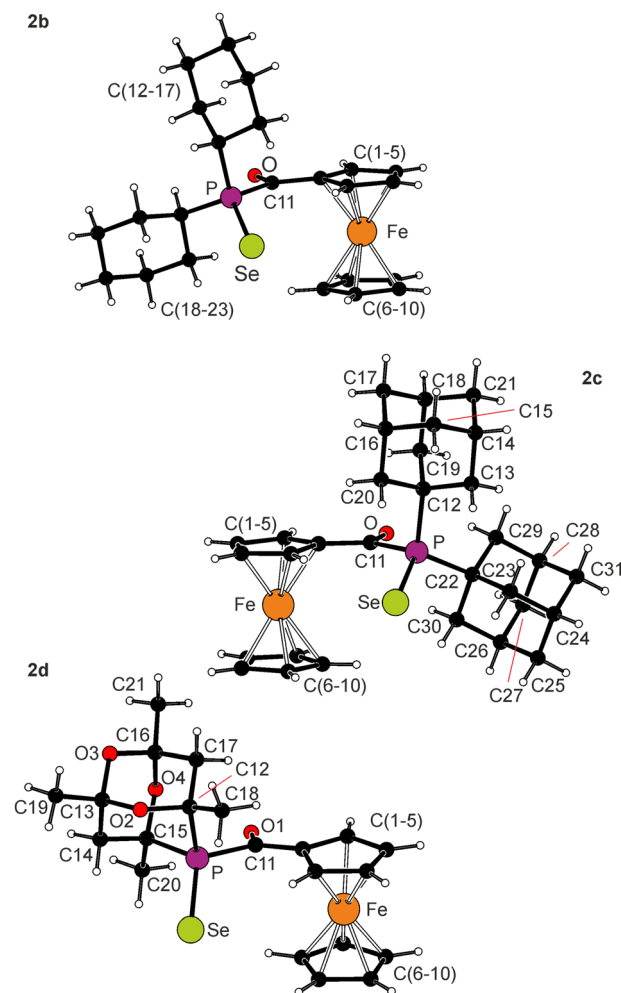


Fig. 3 Molecular structures of **2b–d** (the displacement ellipsoid plots are derived from **1a–d** and related compounds).



Table 2 Selected distances and angles (in Å and deg) for **2b–d**

Parameter ^a	2b	2c	2d^b
Fe–C	2.027(1)–2.059(1)	2.034(2)–2.059(2)	2.024(1)–2.066(2)
Tilt	1.45(7)	2.0(1)	1.92(9)
C11–O	1.222(1)	1.223(2)	1.218(2)
C11–P	1.892(1)	1.908(2)	1.898(1)
P–C ^R	1.840(1)/1.836(1)	1.887(2)/1.890(2)	1.883(1)/1.872(1)
P=Se	2.1124(4)	2.1172(5)	2.0981(5)
C1–C11–P	122.69(8)	122.3(1)	119.56(9)
C ^R –P–C ^R	107.27(5)	113.70(8)	95.34(6)
C ^R –P–C11	102.98(5)/101.54(5)	101.70(8)/104.13(8)	106.52(6)/105.16(6)

^a The tilt is the dihedral angle of the least-squares planes of the cyclopentadienyl rings C(1–5) and C(6–10), and C^R denotes the pivotal carbon atoms of the phosphine substituents for **2b** and **2c** and the C12/C15 atoms for **2d**. ^b The C₃P=Se moiety in the structure of **2d** is disordered, with the P=Se bond exhibiting approximately mirror orientations (97:3). Only data for the more populated orientation are provided.

resonances due to the carbonyl moiety and the ferrocene C^{ipso} (by approximately 12 and 4 ppm, respectively) but only marginally affected the $\nu_{\text{C=O}}$ frequencies (cf. 1612 cm⁻¹ for **3c** and 1606 cm⁻¹ for **1c**).

The crystal structure of **3c**·1.5C₆H₁₂ (Fig. 4) comprises a linear P–Au–Cl moiety (177°) in which the Au–P and Au–Cl distances are similar to those in [AuCl(FcPPh₂)] (Au–P 2.228(2), Au–Cl 2.280(2) Å)¹⁹ and slightly shorter than those in [AuCl(PAD₃)] (Au–P 2.2570(7) Å, Au–Cl 2.2955(7) Å).²⁰ The ferrocene cyclopentadienyls in **3c** are tilted by 4.0(3)°, and the {C11,O,P} moiety deviates from the plane of its bonding cyclopentadienyl ring by 16.0(4)°. Compared to the free ligand **1c**, the P–C(Ad) bonds in the structure of **3c** are 0.01–0.02 Å shorter (the P–C11 bond length remains virtually the same), and the C–P–C angles are 2–3° wider.

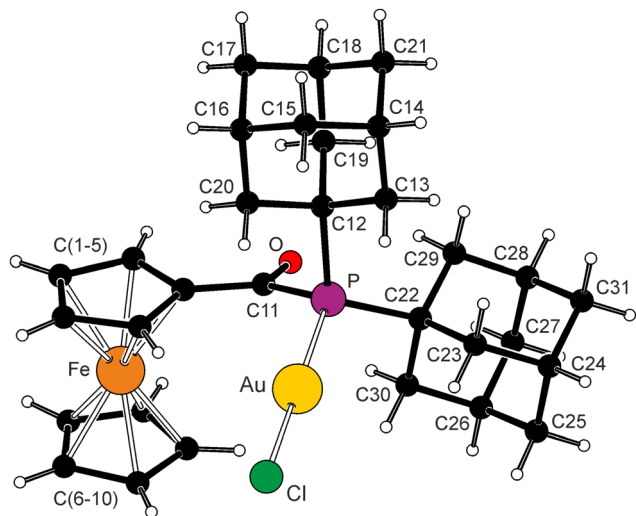
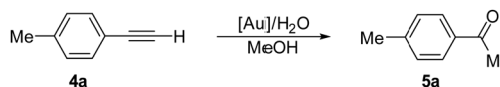


Fig. 4 View of the complex molecule in the structure of **3c**·1.5C₆H₁₂. Selected distances and angles (in Å and deg): Au–P 2.244(1), Au–Cl 2.285(1), P–Au–Cl 177.38(4), Fe–C(1–10) 2.034(4)–2.061(5), C11–O 1.214(6), C1–C11–P 120.7(3), P–C11 1.885(4), P–C12 1.875(4), P–C22 1.871(4), C11–P–C12 100.2(2), C11–P–C22 104.2(2), and C12–P–C22 114.3(2).

Catalytic testing

The complexes **3a–d** were studied as defined precatalysts for gold-mediated reactions.²¹ We initially investigated alkyne hydration, for which gold compounds successfully replaced conventional catalysts (e.g., toxic mercury salts).^{22,23} The hydration reaction is advantageously performed in methanol, which probably first adds to the triple bond to produce a ketal (vinyl ether) intermediate that subsequently hydrolyses to afford the target ketone.²⁴ In our experiments, we also used methanol as the reaction solvent and performed the hydration reaction at a relatively low temperature (40 °C) to effectively differentiate among the performances of the tested catalysts (the typical reaction temperatures are 60–70 °C). Initial screening reactions were performed for the hydration of 4-ethynyltoluene (**4a**) in the presence of complex **3a** (Scheme 4).

Considering the complex role played by Ag(I) ions in hydration catalysis,²⁵ we first attempted to “activate” complex **3a** with sodium salts (4 equiv.). Regrettably, using the catalysts generated from **3a**/Na[BF₄] and **3a**/NaBARF resulted in only poor conversions (at 40 °C for 16 h; see Table 3), presumably due to inefficient halogen removal and, hence, a low concentration of Au(**1a**)⁺ as the plausible active species. Next, we applied silver(I) salts as activating agents. To minimise the influence of these compounds on the reaction course, we used 1 equiv. of a silver salt and activated the gold catalyst separately by mixing with the silver salt and filtering the reaction mixture through a Celite pad to remove the formed AgCl. The use of Ag[BF₄] resulted in a 26% yield of 4-methylacetophenone (**5a**), which further improved upon replacing the silver salt with AgNTf₂ (35%; AgNTf₂ by itself did not catalyse the reaction). Complete conversion was achieved



Scheme 4 Model Au-catalysed alkyne hydration (the reaction conditions are presented in Table 3).

Table 3 Catalytic hydration of alkyne 4-ethynyltoluene (**4a**)^a

Entry	Catalyst	Additive	T [°C]	t [h]	Yield of 5a [%]
1	3a	Na[BF ₄]	40	16	5
2	3a	NaBARF	40	16	6
3	3a	Ag[BF ₄]	40	16	26
4	3a	AgNTf ₂	40	16	35
5	None	AgNTf ₂ ^b	40	16	0
6	3a	AgNTf ₂	60	16	100
7	3a	AgNTf ₂	60	8	72
8	3b	AgNTf ₂	40	16	77
9	3c	AgNTf ₂	40	16	94
10	3d	AgNTf ₂	40	16	13
11	[AuCl(PPh ₃)]	AgNTf ₂	40	16	97
12	[AuCl(FcPPh ₂)]	AgNTf ₂	40	16	97

^a Conditions: substrate **4a** (0.5 mmol) and water (50 μL) were reacted in methanol (1 mL) in the presence of a preformed catalyst (1 mol% Au; see ESI). The yields were determined by integration of ¹H NMR spectra using 4-anisaldehyde as an internal standard and represent the average of two independent runs. NaBARF = Na[B(C₆H₃(CF₃)₂-3,5)₄]. ^b 5 mol% of AgNTf₂ were used.



by increasing the reaction temperature to 60 °C. Halving the reaction time (60 °C/8 h) decreased the yield of **5a** to 72%. No other products were detected in the crude reaction mixture.

When using the remaining complexes **3** under the optimised conditions, the best yield of **5a** was achieved with **3c** as the most electron-rich and bulky ligand, whereas the lowest performance was observed for the complex **3d** featuring the electron-poor, cage phosphine ligand. Notably, all catalysts **3** were outperformed by their conventional analogues, [AuCl(PPh₃)] and [AuCl(FcPPh₂)], which resulted in nearly complete conversion under the same conditions.

The most active complex **3c** was subsequently evaluated in reactions of different substrates (Scheme 5). Replacing the methyl group with an electron-withdrawing trifluoromethyl substituent (substrate **4b**) had a detrimental effect on the reaction yield, affording only 6% of the hydration product **5b**. By contrast, 1-octyne (**4c**) and ethynylferrocene (**4d**) yielded 100 and 65% of the hydration products, respectively. Last, tolane hydration produced ketone **5e** in an 11% yield, in line with the lower reactivity of internal alkynes compared to those of the aforementioned substrates with terminal triple bonds.

The second test reaction was the intramolecular cyclisation of *N*-propargyl benzamide (**6**) to 5-methylene-2-phenyl-4,5-dihydrooxazole (**7**, Scheme 6).²⁶ This reaction was performed under previously reported conditions²⁷ with 1 mol% of the *in situ*-activated Au catalyst in CD₂Cl₂ at 25 °C and monitored by ¹H NMR spectroscopy (Fig. 5). The cyclisation proceeded cleanly and selectively, thereby enabling the yield of **7** to be determined simply by integration of the NMR spectra.

Among the catalysts generated from complexes **3** and AgNTf₂ (1 : 1), the highest yields of 72 and 73% after 1 h reaction time

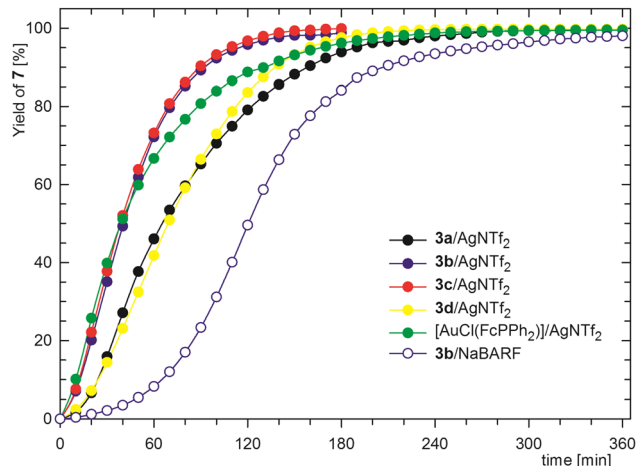
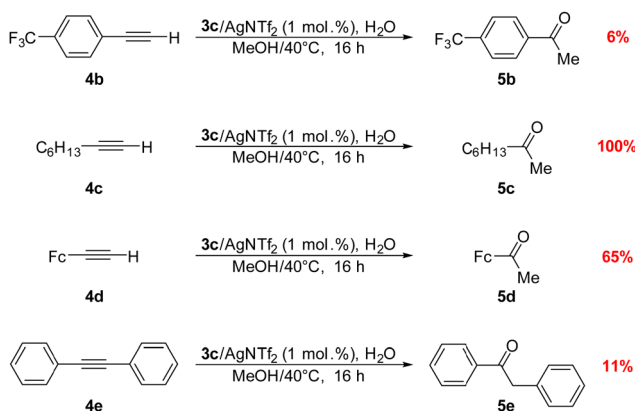


Fig. 5 Kinetic profiles for the Au-catalysed cyclisation of amide **6** (the reaction was performed at 25 °C in CD₂Cl₂ in the presence of 1 mol% Au catalyst; the data are reported as the average of two independent runs).

Table 4 Selected data from kinetic profiles illustrating the catalyst performance^a

Catalyst	Yield of 7 after 1 h [%]	Yield of 7 after 3 h [%]	Time for > 95% conversion [min]
3a	46	94	190
3b	72	99	120
3c	73	100	110
3d	42	98	160
[AuCl(FcPPh ₂)]	67	96	170
3b ^b	8	84	260

^a Au catalyst (1 mol%) generated *in situ* from **3** and AgNTf₂ (1 : 1) was used. The reaction was performed in CD₂Cl₂ (*c*(**6**) = 0.25 M) at 25 °C. ^b NaBARF (2 equiv.) was used instead of the silver salt (as described in the main text).



Scheme 5 Au-catalysed hydration of different alkynes (the reaction conditions are presented in the Experimental section and the footnote to Table 3; the reported yields are the average value from two different runs).



Scheme 6 Gold-catalysed cyclisation of propargyl amide **6**.

(Table 4) were obtained using catalysts based on **3b** and **3c**, respectively, that contained the most electron-rich ligands, whereas yields of 46% and 42% were obtained using catalysts based on **3a** and **3d**. Notably, the kinetic profiles for the catalysts based on **3b** and **3c** were very similar but differed from those for the catalysts containing ligands with lower electron-donating abilities. The yields achieved using the catalysts based on **3a** and **3d** were 79 and 84%, respectively, after 2 h (*i.e.*, the order was inverted from that for the 1 h reaction time) and 94 and 98% for a 3 h reaction time (*N.B.* the reactions with catalysts generated from **3b** and **3c** achieved nearly complete conversions within 2 h). This result can be ascribed to the varying stability of Au(1)⁺ species formed by halide abstraction (reflecting the different abilities of ligands **1** to stabilise such species) and the ease of catalyst activation (the reaction profiles for individual catalysts differ during the first 30 min, showing a gradual reaction acceleration for **3a** and **3d**). The activation of precatalysts **3** appears to be facilitated by phosphine ligands with high electron-donating ability due to their large *trans* influence,²⁸ whereas steric and the electronic characteristics of the auxiliary phosphine ligands appear to control the overall catalyst stability (the differences among the steric properties of **1a**, **b**, **c**, and **d** are



reflected in the estimated buried volume (V_{bur})²⁹ values of 34, 31, 38 and 30%, respectively; see the ESI†).

In agreement with the basicity trend (*vide supra*), the reaction profile obtained using the catalyst produced from [AuCl(FcPPh₂)] fell in between those of **3b/3c** and **3a/3d**. Even in this case, the catalytic species was formed quickly and was highly reactive (a 67% yield was achieved in 1 h) but degraded over time, as shown by the change in the slope of the kinetic profile.

As illustrated for **3b**, using NaBARF to remove the Au-bound chloride instead of the silver salt resulted in significantly slower catalyst activation and slower reaction (Fig. 5). The sigmoidal shape of the kinetic profile during the initial 90 min indicates slow and gradual chloride removal and, together with a slower reaction rate, may suggest equilibria, *e.g.*, between **3a**/NaBARF and Au(**1b**)⁺BARF⁻/NaCl.

Conclusions

In summary, we demonstrated that ferrocene acylphosphines FcC(O)PR₂ are reasonably stable phosphine derivatives that are readily accessible from ferrocenecarboxylic acid and various secondary phosphines R₂PH. Insertion of a carbonyl spacer between the ferrocene unit and the phosphine moiety increases the steric freedom of these compounds and can reduce steric strain in compounds bearing bulky substituents at the phosphorus atom. In addition, the carbonyl group modulates the electronic properties of the terminal phosphine group by counterbalancing the electron-donating properties of the ferrocenyl substituent. These changes in the steric and electronic properties are reflected in the catalytic properties of gold(i) complexes supported with these ligands: substituents with good electron-donating ability and bulky structures may facilitate catalyst activation through halide loss and increase stability of the formed cationic species.

Experimental

Materials and methods

Unless noted otherwise, all syntheses were performed under a nitrogen atmosphere using standard Schlenk techniques. Ferrocenecarboxylic acid,³⁰ 1,3,5,7-tetramethyl-2,4,6-trioxa-8-phosphadamantane (CgPH),^{16b} **1a**⁵ and **6**²⁷ were prepared according to procedures reported in the literature. Other chemicals were purchased from Sigma-Aldrich or TCI and were used as received. Anhydrous dichloromethane, diethyl ether and tetrahydrofuran were obtained using a PureSolv MD5 solvent purification system (Innovative Technology, USA). Triethylamine was distilled from sodium metal and stored under nitrogen. Solvents used during workup and for crystallisation were purchased from Lach-Ner (analytical grade) and used without additional purification.

NMR spectra were recorded at 25 °C on a Varian UNITY Inova 400 spectrometer operating at 399.95, 100.58 and 161.92 MHz for ¹H, ¹³C and ³¹P, respectively. Chemical shifts (δ /ppm) are reported relative to internal SiMe₄ (¹H and ¹³C NMR) and external 85%

aqueous H₃PO₄ (³¹P NMR). FTIR spectra were measured on a Thermo Scientific IS50 instrument in the range of 400–4000 cm⁻¹. Electrospray ionisation mass spectra (ESI MS) were recorded with a Compact QTOF-MS spectrometer (Bruker Daltonics) for samples dissolved in methanol. Elemental analyses were performed on a PE 2400 Series II CHNS/O Elemental Analyser (PerkinElmer).

Synthesis of the acylphosphines **1b–d**

Synthesis of 1b. Oxalyl chloride (1.4 mL, 16 mmol) was added dropwise into a mixture of ferrocenecarboxylic acid (1.61 g, 7.0 mmol) and anhydrous dichloromethane (50 mL) in an oven-dried Schlenk flask, whereupon the solid acid slowly dissolved to give a deep red solution. The mixture was stirred at room temperature for 1 h and then evaporated under vacuum. The crude ferrocenecarbonyl chloride was dissolved in anhydrous diethyl ether (40 mL), and the resulting red solution was cooled on ice and transferred *via* a cannula to an ice-cold solution obtained by mixing dicyclohexylphosphine (1.46 mL, 7.0 mmol) in anhydrous diethyl ether (30 mL) with triethylamine (0.98 mL, 7.0 mmol). A white solid (Et₃NHCl) immediately separated out from the reaction mixture. The resulting mixture was stirred at 0 °C for 30 min and then at room temperature for 3 h, passed through a filter paper and evaporated with chromatographic silica gel (*ca.* 40 mL, size fraction 63–230 μ m). The preadsorbed crude product was transferred onto a silica gel column packed in hexane-ethyl acetate (8 : 1) and eluted with the same solvent mixture. The first red band was collected and evaporated under vacuum to produce pure phosphine **1b** as an amorphous red solid. Yield: 2.67 g (93%).

¹H NMR (CDCl₃, 400 MHz): δ 1.10–1.36 (br m, 10 H, Cy), 1.62–1.86 (br m, 10 H, Cy), 1.94–2.05 (m, 2 H, Cy), 4.23 (s, 5 H, C₅H₅), 4.54 (vt of d, $J' = 2.0, 1.3$ Hz, 2 H, C₅H₄), 4.93 (vt of d, $J' = 2.0, 0.9$ Hz, 2 H, C₅H₄). ¹³C{¹H} NMR (CDCl₃, 101 MHz): δ 26.33 (d, $J_{\text{PC}} = 1$ Hz, Cy), 27.20 (d, $J_{\text{PC}} = 9$ Hz, Cy), 27.34 (d, $J_{\text{PC}} = 10$ Hz, Cy), 29.83 (d, $J_{\text{PC}} = 11$ Hz, Cy), 30.81 (d, $J_{\text{PC}} = 10$ Hz, Cy), 32.37 (d, $J_{\text{PC}} = 13$ Hz, Cy), 69.65 (d, $J_{\text{PC}} = 8$ Hz, CH of C₅H₄), 69.91 (C₅H₅), 72.37 (d, $J_{\text{PC}} = 2$ Hz, CH of C₅H₄), 85.05 (d, $^2J_{\text{PC}} = 39$ Hz, C^{ipso} of C₅H₄), 217.19 (d, $^1J_{\text{PC}} = 41$ Hz, CO). ³¹P{¹H} NMR (CDCl₃, 162 MHz): δ 17.8 (s). IR (DRIFTS, KBr): ν_{max} 3102 w, 3082 w, 2927 s, 2851 m, 1613 s (ν_{CO}), 1441 m, 1370 m, 1338 w, 1293 w, 1243 s, 1199 w, 1181 w, 1108 w, 1056 w, 1037 m, 1027 m, 1001 w, 949 w, 873 w, 850 w, 838 m, 818 m, 744 w, 692 w, 585 w, 549 w, 490 m, 478 m, 444 w cm⁻¹. ESI MS: m/z 433 ([M + Na]⁺), 449 ([M + K]⁺). Anal. calcd for C₂₃H₃₁FeOP (410.3): C 67.33, H 7.62%. Found: C 67.09, H 7.60%.

Synthesis of 1c. The preparation of **1c** was performed similarly but on a smaller scale. Thus, ferrocenecarboxylic acid (460 mg, 2.0 mmol) and oxalyl chloride (0.40 mL, 4.6 mmol) were reacted in anhydrous dichloromethane (20 mL). The acyl chloride was dissolved in diethyl ether (15 mL) and treated with a mixture of di(1-adamantyl)phosphine (639 mg, 2.0 mmol), triethylamine (0.28 mL, 2.0 mmol) and diethyl ether (20 mL). The reaction mixture was stirred overnight and yielded an orange suspension that was evaporated to dryness. The residue was taken up with dichloromethane (50 mL), extracted with water (2 \times 100 mL) and brine (100 mL) and dried over anhydrous



magnesium sulfate. The mixture was filtered and evaporated with chromatographic silica gel. The preadsorbed product was eluted successively with hexane–dichloromethane (5:1) and hexane–dichloromethane (1:1) to remove unreacted di(1-adamantyl) phosphine and, finally, with dichloromethane to elute the product as the only red band, which was collected and evaporated to afford pure **1c** as an orange powdery solid. Yield: 562 mg (54%).

$^1\text{H NMR}$ (CDCl_3 , 400 MHz): δ 1.65–1.76 (m, 12 H, CH_2 of Ad), 1.93 (br s, 6 H, CH of Ad), 2.00–2.10 (m, 12 H, CH_2 of Ad), 4.27 (s, 5 H, C_5H_5), 4.52 (vt of d, $J' = 2.0$, 1.3 Hz, 2 H, C_5H_4), 4.95 (vt of d, $J' = 2.0$, 1.1 Hz, 2 H, C_5H_4). $^{13}\text{C}\{^1\text{H}\}$ NMR (CDCl_3 , 101 MHz): δ 28.91 (d, $^3J_{\text{PC}} = 8$ Hz, CH of Ad), 36.89 (CH_2 of Ad), 38.31 (d, $^1J_{\text{PC}} = 22$ Hz, C^{ipso} of Ad), 41.69 (d, $J_{\text{PC}} = 9$ Hz, CH_2 of Ad), 69.72 (C_5H_5), 70.39 (d, $J_{\text{PC}} = 10$ Hz, CH of C_5H_4), 72.06 (d, $J_{\text{PC}} = 2$ Hz, CH of C_5H_4), 87.57 (d, $^2J_{\text{PC}} = 42$ Hz, C^{ipso} of C_5H_4), 219.05 (d, $^1J_{\text{PC}} = 46$ Hz, CO). $^{31}\text{P}\{^1\text{H}\}$ NMR (CDCl_3 , 162 MHz): δ 45.3 (s). IR (DRIFTS, KBr): ν_{max} 3096 w, 2926 m, 2898 s, 2844 m, 1606 s (ν_{CO}), 1452 m, 1434 m, 1393 w, 1370 m, 1352 m, 1342 m, 1302 w, 1238 s, 1106 m, 1037 m, 1025 m, 1000 w, 970 w, 941 w, 837 w, 822 m, 815 m, 698 m, 588 w, 553 m, 496 m, 487 m, 479 m, 432 w cm^{-1} . ESI MS: m/z 515 ($[\text{M} + \text{H}]^+$), 537 ($[\text{M} + \text{Na}]^+$). Anal. calcd for $\text{C}_{31}\text{H}_{39}\text{FeOP}$ (514.5): C 72.37, H 7.64%. Found: C 72.26, H 7.53%.

Synthesis of 1d. The preparation of **1d** was conducted similarly to that of **1c**, using ferrocenecarboxylic acid (460 mg, 2.0 mmol) and oxalyl chloride (0.40 mL, 4.6 mmol) in anhydrous dichloromethane (20 mL). 1,3,5,7-Tetramethyl-2,4,6-trioxa-8-phosphaadamantane (424 mg, 2.0 mmol) and triethylamine (0.28 mL, 2.0 mmol) were mixed in anhydrous diethyl ether (20 mL) and added to a solution of ferrocenecarbonyl chloride in the same solvent (15 mL). The reaction mixture was stirred overnight and filtered to remove the produced white precipitate, and the filtrate was evaporated. The red oily residue was taken up with hexane–ethyl acetate (8:1), transferred to the top of a chromatographic column and eluted with the same solvent. The first red band was collected and evaporated to give an oily residue, which was diluted with pentane (≈ 5 mL) and stored in a refrigerator. The separated crystals were decanted, washed with cold pentane and dried under vacuum to give **1d** as a red microcrystalline solid. Yield: 146 mg (17%).

$^1\text{H NMR}$ (CDCl_3 , 400 MHz): δ 1.35 (s, 3 H, CH_3), 1.39 (s, 3 H, CH_3), 1.47 (d, $^3J_{\text{PH}} = 12.2$ Hz, 3 H, CH_3), 1.51 (d, $^3J_{\text{PH}} = 13.4$ Hz, 3 H, CH_3), 1.64 (dd, $J = 13.2$, 4.9 Hz, 1 H, CH_2), 1.86 (dd, $J = 24.8$, 13.0 Hz, 1 H, CH_2), 2.05 (dd, $J = 13.0$, 6.5 Hz, 1 H, CH_2), 2.61 (d, $J = 13.2$, 1 H, CH_2), 4.24 (s, 5 H, C_5H_5), 4.58–4.63 (br m, 2 H, C_5H_4), 4.95–4.98 (m, 2 H, C_5H_4). $^{13}\text{C}\{^1\text{H}\}$ NMR (CDCl_3 , 101 MHz): δ 27.78 (CH_3), 27.82 (CH_3), 28.56 (d, $^2J_{\text{PC}} = 10$ Hz, CH_3), 28.90 (d, $^2J_{\text{PC}} = 20$ Hz, CH_3), 37.78 (d, $^2J_{\text{PC}} = 1$ Hz, CH_2), 45.49 (d, $^2J_{\text{PC}} = 16$ Hz, CH_2), 69.48 (d, $J_{\text{PC}} = 7$ Hz, CH of C_5H_4), 70.34 (C_5H_5), 70.35 (d, $J_{\text{PC}} = 10$ Hz, CH of C_5H_4), 72.92 (d, $J_{\text{PC}} = 1$ Hz, CH of C_5H_4), 72.94 (CH of C_5H_4), 73.08 (d, $^1J_{\text{PC}} = 8$ Hz, C^{ipso} of PCg), 74.50 (d, $^1J_{\text{PC}} = 26$ Hz, C^{ipso} of PCg), 85.46 (d, $^2J_{\text{PC}} = 39$ Hz, C^{ipso} of C_5H_4), 96.38 (C^{ipso} of PCg), 96.73 (C^{ipso} of PCg), 213.33 (d, $^1J_{\text{PC}} = 53$ Hz, CO). $^{31}\text{P}\{^1\text{H}\}$ NMR (CDCl_3 , 162 MHz): δ -14.5 (s). IR (DRIFTS, KBr): ν_{max} 3101 w, 3085 w, 2987 w, 2975 w, 2962 w, 2936 w, 2920 w, 2910 w, 1631 m (ν_{CO}),

1615 m (ν_{CO}), 1430 m, 1418 w, 1390 w, 1377 m, 1364 m, 1339 m, 1266 w, 1237 s, 1213 s, 1189 s, 1133 s, 1106 w, 1088 m, 1068 w, 1045 m, 1026 m, 1001 w, 981 s, 965 m, 950 w, 938 m, 897 s, 852 m, 825 s, 814 s, 791 m, 699 m, 686 m, 662 w, 608 w, 574 m, 549 w, 536 m, 498 s, 477 m, 451 w, 437 w cm^{-1} . ESI MS: m/z 451 ($[\text{M} + \text{Na}]^+$), 467 ($[\text{M} + \text{K}]^+$). Anal. calcd for $\text{C}_{21}\text{H}_{25}\text{FeO}_4\text{P}$ (428.2): C 58.90, H 5.88%. Found: C 58.79, H 5.62%.

Preparation of phosphine selenides

Synthesis of 2b. Compound **1b** (82.1 mg, 0.20 mmol) and grey selenium (15.8 mg, 0.21 mmol) were mixed in degassed chloroform (10 mL) in a Schlenk tube. The reaction vessel was sealed and heated to 60 °C in an oil bath overnight under continuous stirring. The reaction mixture was mixed with Celite and filtered through a PTFE syringe filter (0.45 μm porosity), and the filtrate was evaporated under vacuum. The oily residue was dissolved in hot hexane (10 mL) and allowed to crystallise by slow cooling to room temperature. The separated purple crystals were decanted, washed with cold pentane and dried under vacuum. Yield of **2a**: 64.5 mg (66%).

$^1\text{H NMR}$ (CDCl_3 , 400 MHz): δ 1.12–1.53 (br m, 10 H, Cy), 1.65–2.04 (br m, 10 H, Cy), 2.23–2.35 (m, 2 H, Cy), 4.36 (s, 5 H, C_5H_5), 4.68–4.70 (m, 2 H, C_5H_4), 5.51 (vt, $J' = 1.8$ Hz, 2 H, C_5H_4). $^{13}\text{C}\{^1\text{H}\}$ NMR (CDCl_3 , 101 MHz): δ 25.75 (d, $J_{\text{PC}} = 2$ Hz, Cy), 25.99 (d, $J_{\text{PC}} = 1$ Hz, Cy), 26.38 (d, $J_{\text{PC}} = 5$ Hz, Cy), 26.51 (d, $J_{\text{PC}} = 6$ Hz, Cy), 27.17 (d, $J_{\text{PC}} = 3$ Hz, Cy), 36.36 (d, $J_{\text{PC}} = 37$ Hz, Cy), 70.96 (C_5H_5), 71.90 (CH of C_5H_4), 73.73 (CH of C_5H_4), 80.73 (d, $^2J_{\text{PC}} = 50$ Hz, C^{ipso} of C_5H_4), 203.05 (d, $^1J_{\text{PC}} = 35$ Hz, CO). $^{31}\text{P}\{^1\text{H}\}$ NMR (CDCl_3 , 162 MHz): δ 52.3 (s with ^{77}Se satellites, $^1J_{\text{SEP}} = 718$ Hz). IR (DRIFTS, KBr): ν_{max} 2930 s, 2852 m, 1605 s (ν_{CO}), 1450 m, 1435 w, 1410 w, 1371 w, 1350 w, 1258 m, 1107 w, 1052 m, 1030 w, 1002 w, 839 m, 829 m, 746 w, 732 w, 693 w, 587 m, 560 s, 527 w, 499 m, 484 m, 468 m, 448 w cm^{-1} . ESI MS: m/z 513 ($[\text{M} + \text{Na}]^+$). Anal. calcd for $\text{C}_{23}\text{H}_{31}\text{FeOPSe}$ (489.3): C 56.46, H 6.39%. Found: C 56.24, H 6.27%.

Synthesis of 2c. Phosphine **1c** (51.4 mg, 0.10 mmol) and grey selenium (8.7 mg, 0.11 mmol) were reacted in chloroform (5 mL) as described for **2b**. The resulting mixture was filtered through a pad of silica gel and eluted with dichloromethane–methanol (75:1) to give a purple amorphous solid after evaporation. Crystallization by liquid-phase diffusion of hexane into the solution of crude selenide in chloroform produced pure **2c** as purple crystals. Yield: 50 mg (85%).

$^1\text{H NMR}$ (CDCl_3 , 400 MHz): δ 1.65–1.78 (m, 12 H, CH_2 of Ad), 1.95–2.06 (m, 6 H, CH of Ad), 2.18–2.31 (m, 12 H, CH_2 of Ad), 4.36 (s, 5 H, C_5H_5), 4.64 (vt of d, $J' = 2.0$, 0.9 Hz, 2 H, C_5H_4), 5.63 (vt, $J' = 2.0$ Hz, 2 H, C_5H_4). $^{13}\text{C}\{^1\text{H}\}$ NMR (CDCl_3 , 101 MHz): δ 28.70 (d, $^3J_{\text{PC}} = 9$ Hz, CH of Ad), 36.44 (d, $J_{\text{PC}} = 2$ Hz, CH_2 of Ad), 38.49 (d, $J_{\text{PC}} = 2$ Hz, CH_2 of Ad), 43.36 (d, $^1J_{\text{PC}} = 23$ Hz, C^{ipso} of Ad), 70.72 (C_5H_5), 72.69 (CH of C_5H_4), 73.23 (CH of C_5H_4), 82.77 (d, $^2J_{\text{PC}} = 49$ Hz, C^{ipso} of C_5H_4), 205.79 (d, $^1J_{\text{PC}} = 31$ Hz, CO). $^{31}\text{P}\{^1\text{H}\}$ NMR (CDCl_3 , 162 MHz): δ 68.2 (s with ^{77}Se satellites, $^1J_{\text{SEP}} = 709$ Hz). IR (DRIFTS, KBr): ν_{max} 2902 m, 2850 m, 1604 s (ν_{CO}), 1451 w, 1424 w, 1407 w, 1374 w, 1353 w, 1341 w, 1315 w, 1302 w, 1247 m, 1182 w, 1107 w, 1051 m, 1044 m, 1026 w, 1003 w, 973 m, 831 m, 819 m, 696 w, 583 m, 567 m, 532 w,



505 w, 489 m, 478 s, 469 m, 451 m, 430 m cm^{-1} . ESI MS: m/z 617 ($[\text{M} + \text{Na}]^+$). Anal. calcd for $\text{C}_{31}\text{H}_{39}\text{FeOPSe}$ (593.4): C 62.74, H 6.62%. Found: C 62.55, H 6.92%.

Synthesis of 2d. Selenide **2d** was prepared similarly to **2c**, starting from **1d** (42.8 mg, 0.10 mmol) and grey selenium (8.7 mg, 0.11 mmol) in chloroform (5 mL). The reaction mixture was filtered through a pad of silica gel and eluted with dichloromethane–methanol (75:1) to provide a purple amorphous solid after evaporation. The solid was dissolved in chloroform (≈ 1 mL), and the resulting solution was layered with hexane in a test tube. Crystals that formed during several days were decanted, washed with cold pentane and dried under vacuum. Yield of **2d**: 27 mg (53%), purple crystals.

^1H NMR (CDCl_3 , 400 MHz): δ 1.36 (s, 3 H, CH_3), 1.44 (s, 3 H, CH_3), 1.52 (d, $^3J_{\text{PH}} = 15.3$ Hz, 3 H, CH_3), 1.58 (d, $^3J_{\text{PH}} = 14.5$ Hz, 3 H, CH_3), 1.68 (dd, $J = 24.2, 13.7$ Hz, 1 H, CH_2), 2.04 (dd, $J = 20.9, 13.8$ Hz, 1 H, CH_2), 2.57 (dd, $J = 13.8, 1.1$ Hz, 1 H, CH_2), 3.04 (dd, $J = 13.3, 3.6$ Hz, 1 H, CH_2), 4.33 (s, 5 H, C_5H_5), 4.68–4.72 (br m, 2 H, C_5H_4), 5.30 (dtd, $J = 2.6, 1.3, 0.6$ Hz, 1 H, C_5H_4), 5.49 (dt, $J = 2.6, 1.3$ Hz, 1 H, C_5H_4). $^{13}\text{C}\{^1\text{H}\}$ NMR (CDCl_3 , 101 MHz): δ 23.97 (d, $^2J_{\text{PC}} = 2$ Hz, CH_3), 24.08 (d, $^2J_{\text{PC}} = 2$ Hz, CH_3), 27.31 (CH_3), 27.34 (CH_3), 39.36 (d, $^2J_{\text{PC}} = 5$ Hz, CH_2), 40.96 (d, $^2J_{\text{PC}} = 2$ Hz, CH_2), 71.74 (C_5H_5), 72.32 (d, $J_{\text{PC}} = 2$ Hz, CH of C_5H_4), 72.51 (CH of C_5H_4), 73.27 (d, $J_{\text{PC}} = 31$ Hz, C^{ipso} of PCg), 73.54 (CH of C_5H_4), 73.69 (CH of C_5H_4), 76.73 (d, $J_{\text{PC}} = 29$ Hz, C^{ipso} of PCg), 79.59 (d, $^2J_{\text{PC}} = 57$ Hz, C^{ipso} of C_5H_4), 96.57 (d, $^3J_{\text{PC}} = 2$ Hz, C^{ipso} of PCg), 96.63 (d, $^3J_{\text{PC}} = 1$ Hz, C^{ipso} of PCg), 201.61 (d, $J_{\text{PC}} = 27$ Hz, CO). $^{31}\text{P}\{^1\text{H}\}$ NMR (CDCl_3 , 162 MHz): δ 24.2 (s with ^{77}Se satellites, $J_{\text{SEP}} = 761$ Hz). IR (DRIFTS, KBr): ν_{max} 2967 w, 2925 w, 1637 w (ν_{CO}), 1620 m (ν_{CO}), 1453 w, 1431 m, 1412 w, 1394 w, 1381 m, 1373 m, 1364 w, 1345 m, 1323 w, 1262 w, 1248 m, 1213 m, 1202 m, 1183 m, 1136 m, 1106 w, 1090 m, 1047 m, 1034 w, 1006 w, 998 w, 983 s, 959 w, 895 m, 852 m, 839 m, 819 s, 795 m, 702 m, 680 w, 661 w, 635 w, 610 m, 582 m, 568 w, 546 m, 528 w, 503 m, 483 m, 471 m, 445 s, 421 m cm^{-1} . ESI MS: m/z 451 ($[\text{M} - \text{Se} + \text{Na}]^+$), 531 ($[\text{M} + \text{Na}]^+$). Anal. calcd for $\text{C}_{21}\text{H}_{25}\text{FeO}_4\text{PSe}$ (507.2): C 49.73, H 4.97%. Found: C 49.66, H 4.71%.

Synthesis of gold(I) complexes

Synthesis of 3a. Phosphine **1a** (19.9 mg, 0.050 mmol) and $[\text{AuCl}(\text{SMe}_2)]$ (15.0 mg, 0.050 mmol) were dissolved in dry dichloromethane (2 mL) in air. The reaction mixture was stirred for 30 min, filtered through a pad of silica gel and eluted with dichloromethane. The filtrate was evaporated under vacuum, and the residue was dissolved in chloroform (≈ 1 mL). The solution was layered with hexane (4 mL) in a test tube and allowed to crystallise. Purple crystals separated out from the solution overnight and were decanted, washed with cold pentane and dried under vacuum. Yield: 25 mg (80%).

^1H NMR (CDCl_3 , 400 MHz): δ 4.45 (s, 5 H, C_5H_5), 4.70–4.72 (m, 2 H, C_5H_4), 5.15–5.17 (m, 2 H, C_5H_4), 7.46–7.58 (m, 6 H, PPh_2), 7.64–7.72 (m, 4 H, PPh_2). $^{13}\text{C}\{^1\text{H}\}$ NMR (CDCl_3 , 101 MHz): δ 70.98 (d, $J_{\text{PC}} = 4$ Hz, CH of C_5H_4), 71.30 (C_5H_5), 74.48 (d, $J_{\text{PC}} = 1$ Hz, CH of C_5H_4), 78.81 (d, $^2J_{\text{PC}} = 55$ Hz, C^{ipso} of C_5H_4), 126.36 (d, $J_{\text{PC}} = 60$ Hz, C^{ipso} of PPh_2), 129.26 (d, $J_{\text{PC}} = 12$ Hz,

CH of PPh_2), 132.35 (d, $^4J_{\text{PC}} = 3$ Hz, CH^{para} of PPh_2), 134.89 (d, $J_{\text{PC}} = 13$ Hz, CH of PPh_2), 199.78 (d, $^1J_{\text{PC}} = 33$ Hz, CO). $^{31}\text{P}\{^1\text{H}\}$ NMR (CDCl_3 , 162 MHz): δ 29.3 (s). IR (DRIFTS, KBr): ν_{max} 3097 w, 3085 w, 3051 w, 1637 m (ν_{CO}), 1626 s (ν_{CO}), 1571 w, 1479 w, 1436 s, 1410 m, 1372 w, 1350 w, 1328 w, 1314 w, 1252 s, 1186 w, 1103 m, 1050 m, 1028 m, 999 m, 945 w, 870 w, 836 m, 817 m, 750 m, 743 m, 718 w, 691 m, 591 m, 563 m, 515 m, 497 s, 472 m, 456 m cm^{-1} . ESI MS: m/z 653 ($[\text{M} + \text{Na}]^+$). Anal. calcd for $\text{C}_{23}\text{H}_{19}\text{AuClFeOP}$ (630.6): C 43.80, H 3.04%. Found: C 43.57, H 2.94%.

Synthesis of 3b. Phosphine **1b** (20.5 mg, 0.050 mmol) and $[\text{AuCl}(\text{SMe}_2)]$ (15.0 mg, 0.050 mmol) were dissolved in anhydrous dichloromethane (2 mL) without a protective atmosphere. The reaction mixture was stirred for 30 min, filtered through a pad of silica gel and eluted with dichloromethane. The filtrate was evaporated under vacuum, leaving a violet glassy solid, which was dissolved in cyclohexane (≈ 3 mL). A purple microcrystalline solid that separated during several days was isolated by decantation, washed with cold pentane and dried under vacuum to provide pure **3b** as a red crystalline solid. Yield: 24 mg (75%). Crystals used for structure determination were grown from hot cyclohexane.

^1H NMR (CDCl_3 , 400 MHz): δ 1.14–1.52 (br m, 10 H, Cy), 1.66–2.04 (br m, 10 H, Cy), 2.24–2.36 (m, 2 H, Cy), 4.46 (s, 5 H, C_5H_5), 4.76–4.78 (m, 2 H, C_5H_4), 5.30 (vt, $J' = 1.8$ Hz, 2 H, C_5H_4). $^{13}\text{C}\{^1\text{H}\}$ NMR (CDCl_3 , 101 MHz): δ 25.60 (d, $J_{\text{PC}} = 2$ Hz, Cy), 26.52 (d, $J_{\text{PC}} = 12$ Hz, Cy), 26.64 (d, $J_{\text{PC}} = 13$ Hz, Cy), 29.48 (d, $J_{\text{PC}} = 2$ Hz, Cy), 29.88 (s, Cy), 33.23 (d, $J_{\text{PC}} = 31$ Hz, Cy), 70.81 (C_5H_5), 71.18 (d, $J_{\text{PC}} = 3$ Hz, CH of C_5H_4), 74.64 (CH of C_5H_4), 81.68 (d, $^2J_{\text{PC}} = 48$ Hz, C^{ipso} of C_5H_4), 202.05 (d, $J_{\text{PC}} = 27$ Hz, CO). $^{31}\text{P}\{^1\text{H}\}$ NMR (CDCl_3 , 162 MHz): δ 45.0 (s). IR (DRIFTS, KBr): ν_{max} 3202 w, 3087 w, 2927 s, 2850 m, 1614 s (ν_{CO}), 1447 m, 1436 m, 1411 w, 1373 m, 1352 w, 1329 w, 1292 w, 1258 s, 1199 w, 1180 w, 1171 w, 1106 w, 1052 m, 1031 m, 1003 m, 948 w, 915 w, 888 w, 851 m, 838 m, 823 m, 752 w, 730 w, 693 w, 584 w, 561 m, 500 s, 486 m, 468 m, 444 m, 429 w cm^{-1} . ESI MS: m/z 665 ($[\text{M} + \text{Na}]^+$). Anal. calcd for $\text{C}_{23}\text{H}_{31}\text{AuClFeOP}$ (642.7): C 42.98, H 4.86%. Found: C 43.02, H 4.49%.

Synthesis of 3c. Compound **3c** was prepared similarly from **1c** (25.7 mg, 0.050 mmol) and $[\text{AuCl}(\text{SMe}_2)]$ (15.0 mg, 0.050 mmol). Crystallisation from cyclohexane (≈ 2 mL) afforded the solvate **3c**· C_6H_{12} as purple crystals. Yield: 36 mg (84%).

^1H NMR (CDCl_3 , 400 MHz): δ 1.68–1.80 (m, 12 H, CH_2 of Ad), 2.00–2.07 (m, 6 H, CH of Ad), 2.18–2.32 (m, 12 H, CH_2 of Ad), 4.46 (s, 5 H, C_5H_5), 4.74 (vt of d, $J' = 2.0$ Hz, 1.2 Hz, 2 H, C_5H_4), 5.39 (vt, $J' = 1.8$ Hz, 2 H, C_5H_4). $^{13}\text{C}\{^1\text{H}\}$ NMR (CDCl_3 , 101 MHz): δ 28.58 (d, $^3J_{\text{PC}} = 9$ Hz, CH of Ad), 36.26 (d, $J_{\text{PC}} = 1$ Hz, CH_2 of Ad), 41.63 (CH_2 of Ad), 42.65 (d, $J_{\text{PC}} = 20$ Hz, C^{ipso} of Ad), 70.65 (C_5H_5), 71.86 (d, $J_{\text{PC}} = 3$ Hz, CH of C_5H_4), 74.26 (CH of C_5H_4), 83.78 (d, $^2J_{\text{PC}} = 46$ Hz, C^{ipso} of C_5H_4), 204.96 (d, $J_{\text{PC}} = 21$ Hz, CO). $^{31}\text{P}\{^1\text{H}\}$ NMR (CDCl_3 , 162 MHz): δ 64.1 (s). IR (DRIFTS, KBr): ν_{max} 2905 s, 2850 m, 1612 s (ν_{CO}), 1449 m, 1429 m, 1371 w, 1353 w, 1343 m, 1300 w, 1249 m, 1107 w, 1047 m, 1026 w, 1000 w, 972 w, 837 m, 826 m, 696 w, 587 w, 565 m, 521 w, 506 w, 489 m, 479 s, 464 m, 451 m, 430 m cm^{-1} . ESI MS: m/z 769 ($[\text{M} + \text{Na}]^+$). Anal. calcd for $\text{C}_{31}\text{H}_{39}\text{AuClFeOP}\cdot\text{C}_6\text{H}_{12}$ (831.0): C 53.47, H 6.19%. Found: C 53.42, H 5.97%.



Synthesis of 3d. The procedure described above was followed starting from **1d** (21.2 mg, 0.050 mmol) and [AuCl(SMe₂)] (15.0 mg, 0.050 mmol). The crude product was dissolved in ethyl acetate (\approx 2 mL), and the solution was allowed to stand for 1 h, during which time a purple solid was rapidly deposited. The separated solid was carefully decanted and washed with cold pentane to give **3d**. Yield: 25 mg (76%), purple powdery solid.

¹H NMR (CDCl₃, 400 MHz): δ 1.38 (s, 3 H, CH₃), 1.44 (s, 3 H, CH₃), 1.58 (d, ³J_{PH} = 8.1 Hz, 3 H, CH₃), 1.62 (d, ³J_{PH} = 9.6 Hz, 3 H, CH₃), 1.84 (dd, J = 25.5 Hz, 13.6 Hz, 1 H, CH₂), 1.96 (dd, J = 16.9 Hz, 13.8 Hz, 1 H, CH₂), 2.50 (dd, J = 13.7 Hz, 4.5 Hz, 1 H, CH₂), 2.51 (dd, J = 13.7 Hz, 0.9 Hz, 1 H, CH₂), 4.47 (s, 5 H, C₅H₅), 4.79–4.85 (br m, 2 H, C₅H₄), 5.21–5.24 (m, 1 H, C₅H₄), 5.38–5.40 (m, 1 H, C₅H₄). ¹³C{¹H} NMR (CDCl₃, 101 MHz): δ 27.07 (d, ²J_{PC} = 4 Hz, CH₃), 27.27 (CH₃), 27.30 (CH₃), 28.05 (d, ²J_{PC} = 7 Hz, CH₃), 38.60 (d, ²J_{PC} = 1 Hz, CH₂), 44.68 (d, ²J_{PC} = 8 Hz, CH₂), 70.99 (d, J_{PC} = 4 Hz, CH of C₅H₄), 71.40 (C₅H₅), 71.54 (d, J_{PC} = 3 Hz, CH of C₅H₄), 74.25 (d, ¹J_{PC} = 30 Hz, C^{ipso} of PCg), 74.78 (d, J_{PC} = 2 Hz, CH of C₅H₄), 75.10 (CH of C₅H₄), 75.11 (d, ¹J_{PC} = 23 Hz, C^{ipso} of PCg), 81.37 (d, ²J_{PC} = 52 Hz, C^{ipso} of C₅H₄), 96.66 (d, ³J_{PC} = 2 Hz, C^{ipso} of PCg), 97.05 (C^{ipso} of PCg), 199.05 (d, ¹J_{PC} = 12 Hz, CO). ³¹P{¹H} NMR (CDCl₃, 162 MHz): δ 16.0 (s). IR (DRIFTS, KBr): ν_{\max} 3086 w, 2999 w, 2974 w, 2963 w, 2921 w, 1632 m (ν_{CO}), 1617 (ν_{CO}), 1450 w, 1436 m, 1394 w, 1385 w, 1373 w, 1346 w, 1249 m, 1231 w, 1216 m, 1205 m, 1187 m, 1135 m, 1109 w, 1088 m, 1048 m, 1035 w, 1004 w, 983 s, 961 w, 940 w, 893 m, 855 m, 836 s, 813 m, 792 m, 703 w, 683 m, 605 m, 579 m, 546 m, 516 w, 495 s, 487 m, 463 m, 443 s cm⁻¹. ESI MS: m/z 683 ([M + Na]⁺). Anal. calcd for C₂₁H₂₅AuClFeO₄P (660.7): C 38.18, H 3.81%. Found: C 37.89, H 3.58%.

Catalytic experiments

Hydration of 4-ethynyltoluene. The appropriate complex **3** (0.0050 mmol) was dissolved in dichloromethane (0.5 mL) in a vial. A freshly prepared solution of a silver(i) salt (0.50 mL of a 10 mM methanol solution, 0.0050 mmol) was introduced to the aforementioned solution, and the mixture was stirred for 30 min. Next, the mixture was mixed with a small quantity of Celite and filtered through a PTFE syringe (0.45 μ m porosity), and the filtrate was evaporated in a Schlenk tube. Deionised water (50 μ L), 4-ethynyltoluene (**4a**; 60 mg, 0.50 mmol) and anhydrous methanol (1 mL) were introduced into the filtrate, and the reaction vessel was transferred to a preheated oil bath and stirred for the given time. The reaction was terminated by the addition of brine (5 mL) and deionised water (1 mL). The internal standard 4-anisaldehyde (68 mg, 0.50 mmol) and CDCl₃ (0.5 mL) were added to the mixture, followed by extraction. The organic phase was separated and filtered through a syringe filter directly into a 5 mm NMR tube. The yield was determined by comparison of the signals generated by the methoxy group of the internal standard (δ_{H} 3.83 ppm) and MeC₆H₄ of the product (δ_{H} 2.38 ppm) or the acyl resonance MeCO (δ_{H} 2.54 ppm).

4-Methylacetophenone (5a).³¹ ¹H NMR (CDCl₃, 400 MHz): δ 2.38 (s, 3 H, CH₃C₆H₄), 2.55 (s, 3 H, CH₃CO), 7.23 (d, J = 7.6 Hz, 2 H, C₆H₄), 7.83 (d, J = 7.6 Hz, 2 H, C₆H₄).

4-Trifluoromethylacetophenone (5b).³² ¹H NMR (CDCl₃, 400 MHz): δ 2.63 (s, 3 H, CH₃CO), 7.71 (d, J = 7.9 Hz, 2 H, C₆H₄), 8.04 (d, J = 8.0 Hz, 2 H, C₆H₄).

2-Octanone (5c).³³ ¹H NMR (CDCl₃, 400 MHz): δ 0.88 (t, J = 6.8 Hz, 3 H, CH₃), 1.23–1.35 (m, 6 H, 3 \times CH₂), 1.52–1.61 (m, 2 H, CH₂), 2.13 (s, 3 H, CH₃CO), 2.42 (t, J = 7.5 Hz, 2 H, CH₂CO).

Acetylferrocene (5d).³⁴ ¹H NMR (CDCl₃, 400 MHz): δ 2.37 (s, 3 H, CH₃CO), 4.18 (s, 5 H, C₅H₅), 4.48 (vt, J' = 2.0 Hz, 2 H, C₅H₄), 4.75 (vt, J' = 2.0 Hz, 2 H, C₅H₄).

1,2-Diphenylethanone (5e).³⁵ ¹H NMR (CDCl₃, 400 MHz): δ 4.23 (s, 2 H, CH₂CO), 7.15–7.32 (m, 5 H, Ph), 7.36–7.44 (m, 2 H, Ph), 7.46–7.55 (m, 1 H, Ph), 7.93–7.99 (m, 2 H, Ph).

Cyclisation of *N*-propargyl benzamide. Solid *N*-propargyl benzamide (**6**; 31.8 mg, 0.20 mmol) and silver(i) bis(trifluoromethanesulfonyl)imide (0.77 mg, 0.0020 mmol) were dissolved in CD₂Cl₂ (0.8 mL), and the solution was poured onto the solid gold(i) precatalyst (0.0020 mmol, 1 mol%). After two minutes, the solution was filtered through a PTFE syringe (0.45 μ m porosity) into an NMR tube, which was inserted into the NMR spectrometer. The first spectrum was acquired 10 minutes after mixing all starting materials, and subsequent spectra were recorded every 10 minutes for six hours. The yield was determined by comparing the integral intensities of the NCH₂ signals due to the substrate (δ_{H} 4.21 ppm) and the cyclisation product (δ_{H} 4.63 ppm).

5-Methylene-2-phenyl-4,5-dihydrooxazole (7).²⁷ ¹H NMR (400 MHz, CD₂Cl₂): δ = 4.37 (q, $J \approx$ 2.6 Hz, 1 H, =CHH), 4.63 (t, ⁴J_{HH} \approx 2.8 Hz, 2 H, NCH₂), 4.79 (q, $J \approx$ 2.9 Hz, 1 H, =CHH), 7.41–7.48 (m, 2 H, CH of C₆H₅), 7.49–7.55 (m, 1 H, CH of C₆H₅), 7.93–7.99 (m, 2 H, CH of C₆H₅).

X-ray crystallography

Diffraction data were recorded at 120 or 150 K with a Bruker D8 VENTURE Kappa Duo diffractometer with a PHOTON III detector and a Cryostream Cooler (Oxford Cryosystems) using Cu K α (λ = 1.54178 Å for **1b**) or Mo K α radiation (λ = 0.71073 Å for all other compounds). The structures were solved by direct methods (SHELXT, recent version³⁶) and subsequently refined by a full-matrix least-squares routine based on F^2 (SHELXL-2014/2017³⁷). All nonhydrogen atoms were refined with anisotropic displacement parameters, and the hydrogen atoms were placed in their theoretical positions and refined as riding atoms using the standard parameters implemented in SHELXL.

Compound **2c** formed partially disordered crystals with the P=Se bonds occupying approximately mirror-image positions within the space defined by the bulky adamantyl substituents. The refined occupancies for the two orientations were 97:3. Furthermore, the crystals of **1b** and **3c**·1.5C₆H₁₂ were nonmerohedral, two-component twins. The refined contributions from the two crystal domains were approximately 70:30 for **1b** and 51:49 for **3c**·1.5C₆H₁₂.

Selected crystallographic data and structure refinement parameters are available in the ESI† (Table S1). The geometric data and structural diagrams were obtained using a recent version of the PLATON program.³⁸ All numerical values were



rounded to one decimal place with respect to their estimated standard deviations.

Conflicts of interest

There are no conflicts to declare.

Acknowledgements

The Czech Science Foundation is acknowledged for financial support (project No. 19-09334S). The authors thank Dr Ivana Císařová of the Department of Inorganic Chemistry, Faculty of Science, Charles University, for recording the X-ray diffraction data.

References

- 1 P. Kumar, U. Sharma and G. S. Ananthnag, *Appl. Organomet. Chem.*, 2022, **36**, e6672.
- 2 For examples, see: (a) J. Li, C. Yang, Y. Bai, X. Yang, Y. Liu and J. Peng, *J. Organomet. Chem.*, 2018, **855**, 7; (b) J. Yang, X. Chen and Z. Wang, *Tetrahedron Lett.*, 2015, **56**, 5673; (c) P. Kumar, M. M. Siddiqui, Y. Reddi, J. T. Mague, R. B. Sunoj and M. S. Balakrishna, *Dalton Trans.*, 2013, **42**, 11385; (d) S. Gowrisankar, H. Neumann, A. Spannenberg and M. Beller, *Organometallics*, 2014, **33**, 94; (e) S. Gowrisankar, C. Federsel, H. Neumann, C. Ziebart, R. Jackstell, A. Spannenberg and M. Beller, *ChemSusChem*, 2013, **6**, 85; (f) R. A. Baber, M. L. Clarke, A. G. Orpen and D. A. Ratcliffe, *J. Organomet. Chem.*, 2003, **667**, 112.
- 3 (a) In *Ferrocenes: Homogeneous Catalysis, Organic Synthesis, Materials Science*, ed. A. Togni and T. Hayashi, VCH, Weinheim, 1995; (b) In *Ferrocenes: Ligands, Materials and Biomolecules*, ed. P. Štěpnička, Wiley, Chichester, 2008; (c) R. C. J. Atkinson, V. C. Gibson and N. J. Long, *Chem. Soc. Rev.*, 2004, **33**, 313; (d) R. Gómez Arrayás, J. Adrio and J. C. Carretero, *Angew. Chem., Int. Ed.*, 2006, **45**, 7674; (e) L. Cunningham, A. Benson and P. J. Guiry, *Org. Biomol. Chem.*, 2020, **18**, 9329; (f) P. Štěpnička, *Dalton Trans.*, 2022, **51**, 8085.
- 4 E. Fuchs, B. Breit, H. Heydt, M. Regitz, W. Schoeller, T. Busch, C. Krüger and P. Betz, *Chem. Ber.*, 1991, **124**, 2843.
- 5 R. Pietschnig, E. Niecke, M. Nieger and K. Airola, *J. Organomet. Chem.*, 1997, **529**, 127.
- 6 P. Vosáhló, J. Schulz, I. Císařová and P. Štěpnička, *Dalton Trans.*, 2021, **50**, 6232.
- 7 P. Vosáhló, I. Císařová and P. Štěpnička, *New J. Chem.*, 2022, **46**, 21536.
- 8 (a) K.-S. Gan and T. S. A. Hor, in *Ferrocenes: Homogeneous Catalysis, Organic Synthesis Materials Science*, ed. A. Togni and T. Hayashi, Wiley-VCH, Weinheim, Germany, 1995, ch. 1, pp. 3–104; (b) S. W. Chien and T. S. A. Hor, in *Ferrocenes: Ligands, Materials and Biomolecules*, ed. P. Štěpnička, Wiley, Chichester, UK, 2008, ch. 2, pp. 33–116; (c) T. J. Colacot and S. Parisel, in *Ferrocenes: Ligands, Materials and Biomolecules*, ed. P. Štěpnička, Wiley, Chichester, UK, 2008, ch. 3, pp. 117–140; (d) G. Bandoli and A. Dolmella, *Coord. Chem. Rev.*, 2000, **209**, 161; (e) S. Dey and R. Pietschnig, *Coord. Chem. Rev.*, 2021, **437**, 213850.
- 9 H. Shet, U. Parmar, S. Bhilare and A. R. Kapdi, *Org. Chem. Front.*, 2021, **8**, 1599.
- 10 (a) F. Horký, I. Císařová and P. Štěpnička, *ChemCatChem*, 2021, **13**, 4848; (b) F. Horký, I. Císařová and P. Štěpnička, *J. Organomet. Chem.*, 2022, **957**, 122145.
- 11 B. Breit and D. Breuninger, *Synthesis*, 2005, 2782.
- 12 (a) Z. Szarka, R. Skoda-Földes, Á. Kuik, Z. Berente and L. Kollár, *Synthesis*, 2003, 545; (b) C. Lu, X. Wang, Y. Yang and X. Liu, *Inorg. Chim. Acta*, 2016, **447**, 121.
- 13 C. A. Tolman, *Chem. Rev.*, 1977, **77**, 313.
- 14 U. Beckmann, D. Süslüyan and P. C. Kunz, *Phosphorus, Sulfur Silicon Relat. Elem.*, 2011, **186**, 2061.
- 15 R. P. Pinnell, C. A. Megerle, S. L. Manatt and P. A. Kroon, *J. Am. Chem. Soc.*, 1973, **95**, 977.
- 16 (a) C. Hansch, A. Leo and R. W. Taft, *Chem. Rev.*, 1991, **91**, 165; (b) J. H. Downing, J. Floure, K. Heslop, M. F. Haddow, J. Hopewell, M. Lusi, H. Phetmung, A. G. Orpen, P. G. Pringle, R. I. Pugh and D. Zambrano-Williams, *Organometallics*, 2008, **27**, 3216.
- 17 B. Milde, M. Lohan, C. Schreiner, T. Ruffer and H. Lang, *Eur. J. Inorg. Chem.*, 2011, 5437.
- 18 The data were taken from: (a) A. Muller, S. Otto and A. Roodt, *Dalton Trans.*, 2008, 650; (b) M. L. Kelty, A. J. McNeece, J. W. Kurutz, A. S. Filatov and J. S. Anderson, *Chem. Sci.*, 2022, **13**, 4377 and refs. 14 and 17.
- 19 K. Rössler, T. Ruffer, B. Walfort, R. Packheiser, R. Holze, M. Zharnikov and H. Lang, *J. Organomet. Chem.*, 2007, **692**, 1530.
- 20 L. Chen, P. Ren and B. P. Carrow, *J. Am. Chem. Soc.*, 2016, **138**, 6392.
- 21 (a) A. S. K. Hashmi, *Chem. Rev.*, 2007, **107**, 3180; (b) R. Dorel and A. M. Echavarren, *Chem. Rev.*, 2015, **115**, 9028.
- 22 L. Hintermann and A. Labonne, *Synthesis*, 2007, 1121.
- 23 For the first report of applications of Au(I) compounds in alkyne hydration, see: E. Mizushima, K. Sato, T. Hayashi and M. Tanaka, *Angew. Chem., Int. Ed.*, 2002, **41**, 4563.
- 24 A. Leyva and A. Corma, *J. Org. Chem.*, 2009, **74**, 2067.
- 25 On the one hand, silver(I) salts are commonly used to generate active species of the type LAu⁺ from stable precursors [LAuCl]. On the other hand, formation of relatively stable, geminally dimetallated intermediates, R₂C = C(AuL)(AgL_n), can slow the Au-mediated reaction: (a) D. Weber and M. R. Gagné, *Org. Lett.*, 2009, **11**, 4962; (b) D. Wang, R. Cai, S. Sharma, J. Jirak, S. K. Thummanapelli, N. G. Akhmedov, H. Zhang, X. Liu, J. L. Petersen and X. Shi, *J. Am. Chem. Soc.*, 2012, **134**, 9012.
- 26 (a) A. S. K. Hasmi, J. P. Weyrauch, W. Frey and J. W. Bats, *Org. Lett.*, 2004, **6**, 4391; (b) J. P. Weyrauch, A. S. K. Hashmi, A. Schuster, T. Hengst, S. Schetter, A. Littmann, M. Rudolph, M. Hamzic, J. Visus, F. Rominger, W. Frei and J. W. Bats, *Chem. – Eur. J.*, 2010, **16**, 956.
- 27 O. Bárta, I. Císařová, J. Schulz and P. Štěpnička, *New J. Chem.*, 2019, **43**, 11258.
- 28 (a) P. G. Jones and A. F. Williams, *J. Chem. Soc., Dalton Trans.*, 1977, 1430; (b) P. G. Jones, A. G. Maddock,



- M. J. Mays, M. M. Muir and A. F. Williams, *J. Chem. Soc., Dalton Trans.*, 1977, 1434.
- 29 (a) L. Falivene, Z. Cao, A. Petta, L. Serra, A. Poater, R. Oliva, V. Scarano and L. Cavallo, *Nat. Chem.*, 2019, **11**, 872; (b) L. Falivene, R. Cudendino, A. Poater, A. Petta, L. Serra, R. Oliva, V. Scarano and L. Cavallo, *Organometallics*, 2016, **35**, 2286.
- 30 P. C. Reeves, J. J. Mrowca, M. M. Borecki and W. A. Sheppard, *Org. Synth.*, 1977, **56**, 28.
- 31 Y. Yang, A. Qin, K. Zhao, D. Wang and X. Shi, *Adv. Synth. Catal.*, 2016, **358**, 1433.
- 32 H. Morimoto, T. Tsubogo, N. D. Litvinas and J. F. Hartwig, *Angew. Chem., Int. Ed.*, 2011, **50**, 3793.
- 33 R. E. Ebule, D. Malhotra, G. B. Hammond and B. Xu, *Adv. Synth. Catal.*, 2016, **358**, 1478.
- 34 V. A. Darin, A. F. Neto, J. Miller, M. M. F. Afonso, H. C. Fonsatti and Á. D. L. Borges, *J. Prakt. Chem.*, 1999, **341**, 588.
- 35 A. Rühling, H.-J. Galla and F. Glorius, *Chem. – Eur. J.*, 2015, **21**, 12291.
- 36 G. M. Sheldrick, *Acta Crystallogr., Sect. A: Found. Adv.*, 2015, **71**, 3.
- 37 G. M. Sheldrick, *Acta Crystallogr., Sect. C: Struct. Chem.*, 2015, **71**, 3.
- 38 (a) A. L. Spek, *J. Appl. Crystallogr.*, 2003, **36**, 7; (b) A. L. Spek, *Acta Crystallogr., Sect. D: Biol. Crystallogr.*, 2009, **65**, 148.

